Research Article

Rapid Communications in Mass Spectrometry

Received: 7 May 2014 Revised: 20 August 2014 Accepted: 24 August 2014 Published online in Wiley Online Library

Rapid Commun. Mass Spectrom. **2014**, *28*, 2325–2336
(wileyonlinelibrary.com) DOI: 10.1002/rcm.7028

Desorption atmospheric pressure photoionization and direct analysis in real time coupled with travelling wave ion mobility mass spectrometry

Riikka-Marjaana Räsänen[1,2], Prabha Dwivedi[2,3,4†], Facundo M. Fernández[2,3*] and Tiina J. Kauppila[1]**

[1]Division of Pharmaceutical Chemistry and Technology, Faculty of Pharmacy, University of Helsinki, P.O. Box 56, 00014, Helsinki, Finland
[2]School of Chemistry and Biochemistry, Georgia Institute of Technology, 901 Atlantic Drive NW, Atlanta, GA 30332, USA
[3]Center for Chemical Evolution, Georgia Institute of Technology, 901 Atlantic Drive NW, Atlanta, GA 30332, USA
[4]Centres for Disease Control and Prevention, 4770 Buford Highway, Atlanta, GA 30341, USA

RATIONALE: Ambient mass spectrometry (MS) is a tool for screening analytes directly from sample surfaces. However, background impurities may complicate the spectra and therefore fast separation techniques are needed. Here, we demonstrate the use of travelling wave ion mobility spectrometry in a comparative study of two ambient MS techniques.
METHODS: Desorption atmospheric pressure photoionization (DAPPI) and direct analysis in real time (DART) were coupled with travelling wave ion mobility mass spectrometry (TWIM-MS) for highly selective surface analysis. The ionization efficiencies of DAPPI and DART were compared. Test compounds were: bisphenol A, benzo[a]pyrene, ranitidine, cortisol and α-tocopherol. DAPPI-MS and DART-TWIM-MS were also applied to the analysis of chloroquine from dried blood spots, and α-tocopherol from almond surface, and DAPPI-TWIM-MS was applied to analysis of pharmaceuticals and multivitamin tablets.
RESULTS: DAPPI was approximately 100 times more sensitive than DART for bisphenol A and 10–20 times more sensitive for the other compounds. The limits of detection were between 30–290 and 330–8200 fmol for DAPPI and DART, respectively. Also, from the authentic samples, DAPPI ionized chloroquine and α-tocopherol more efficiently than DART. The mobility separation enabled the detection of species with low signal intensities, e.g. thiamine and cholecalciferol, in the DAPPI-TWIM-MS analysis of multivitamin tablets.
CONCLUSIONS: DAPPI ionized the studied compounds of interest more efficiently than DART. For both DAPPI and DART, the mobility separation prior to MS analysis reduced the amount of chemical noise in the mass spectrum and significantly increased the signal-to-noise ratio for the analytes.

Ambient mass spectrometry (MS) techniques allow the rapid sampling and ionization of compounds of interest directly from solid or liquid samples, without prior sample pretreatment.[1] During the last ten years, tens of different ambient ionization techniques have been introduced. The most popular techniques according to the number of publications are desorption electrospray ionization (DESI)[2] and direct analysis in real time (DART).[3] In DESI, the sample is sprayed with a jet of charged solvent, which forms a thin film on the sample surface. The analytes are rapidly dissolved and carried away by the continuous solvent jet in the form of secondary droplets into the mass spectrometer.[4,5] From the droplets, the analyte ions are mainly formed by electrospray ionization (ESI) mechanisms,[6–8] but also gas-phase ion-molecule reactions have been suggested.[9] DESI has proven to be a sensitive method for polar and high mass weight compounds.[10] However, the sensitivity of DESI for neutral and low polarity compounds, such as fat-soluble vitamins and steroids, is low.[11]

In DART, the sample is placed between the exit capillary of the ion source and the mass spectrometer, and exposed to a heated gas flow of metastable atoms or molecules (N*) generated by a discharge between two electrodes. The gas flow desorbs and ionizes sample compounds from the surface, and the formed ions are directed to the MS inlet capillary. Ion formation has been suggested to start with

* *Correspondence to:* F. M. Fernández, School of Chemistry and Biochemistry, Georgia Institute of Technology, 901 Atlantic Drive NW, Atlanta, GA 30332, USA.
E-mail: facundo.fernandez@chemistry.gatech.edu
** *Correspondence to:* T. J. Kauppila, Division of Pharmaceutical Chemistry and Technology, Faculty of Pharmacy, University of Helsinki, P.O. Box 56, 00014 Helsinki, Finland.
E-mail: tiina.kauppila@helsinki.fi
† Present address: Centres for Disease Control and Prevention, 4770 Buford Highway, Atlanta, GA 30341, USA.

Penning ionization, where N* reacts with gas-phase molecules forming a molecular ion $M^{+\bullet}$ and releasing an electron (reaction (1)).[3,12,13]

$$N^* + M \rightarrow N + M^{+\bullet} + e^- \quad (1)$$

This will happen if the ionization energy (IE) of M is lower than the internal energy of N*. Since helium (He) is typically used in DART and the internal energy of the most abundant He metastable species is 19.8 eV, both atmospheric water (IE 12.62 eV) and oxygen (IE 12.07 eV) can be efficiently ionized. This first Penning ionization step of atmospheric water eventually results in the formation of protonated water clusters, $[(H_2O)_n + H]^+$, which may react with analyte (A) or sample solvent (S) molecules[13] through proton transfer reactions (reaction (2)).

$$\left[(H_2O)_n + H\right]^+ + (A \text{ or } S_n) \rightarrow [(A \text{ or } S_n) + H]^+ + (H_2O)_n \quad (2)$$

Protonated solvent species may also be generated when $M^{+\bullet}$ (in reaction (1)) is a solvent molecular ion ($S^{+\bullet}$), which can further undergo proton transfer reactions with other solvent molecules forming $[S_n + H]^+$. This species can also react with the analytes through proton transfer (reaction (3)). $S^{+\bullet}$ can also ionize the analytes through charge exchange, forming $A^{+\bullet}$ (reaction (4)), or through proton transfer forming protonated analyte molecules (reaction (5)).[13]

$$[S_n + H]^+ + A \rightarrow S_n + [A + H]^+ \quad (3)$$

$$S^{+\bullet} + A \rightarrow S + A^{+\bullet} \quad (4)$$

$$S^{+\bullet} + A \rightarrow [S - H]^\bullet + [A + H]^+ \quad (5)$$

Unlike DESI, DART is not so readily applied to large molecules with low volatility, because heat is used to assist in the desorption process.

In desorption atmospheric pressure photoionization (DAPPI) a heated solvent jet is focused on the sample, causing thermal desorption of compounds from the sample surface.[14] Ionization takes place in the gas phase by reactions similar to those in atmospheric pressure photoionization (APPI).[15] The process is initiated by 10 eV photons emitted by a vacuum ultraviolet (VUV) lamp. Typically, dopant (D), a solvent that can be directly ionized by the 10 eV photons, is used to produce reactant ions (reaction (6)). These reactant ions can ionize the analytes (A) either through charge exchange or proton transfer (reactions (7) and (8), respectively).

$$D + h\nu \rightarrow D^{+\bullet} + e^- \quad (6)$$

$$D^{+\bullet} + A \rightarrow A^{+\bullet} + D \quad (7)$$

$$D^{+\bullet} + A \rightarrow [D - H]^\bullet + [A + H]^+ \quad (8)$$

As in DART, the IE and proton affinity (PA) values play key roles in DAPPI. In theory, direct ionization of analytes with IE <10 eV is possible, but it has been shown to be far less efficient than the dopant-assisted pathway.[16] Ionization via charge exchange depends on the IE of the compound rather than the PA, and therefore nonpolar compounds with low PAs can be ionized efficiently by DAPPI.[14] In a comparative study of DAPPI and DESI, DAPPI showed significantly better tolerance towards biological sample matrices than DESI.[17] DAPPI has also shown better sensitivity for polyaromatic hydrocarbons,[18] low polarity lipids,[11] fat-soluble vitamins[11] and steroids[11,14] than DESI. Comparative benchmarking studies between DAPPI and DART have thus far not been performed, although both techniques are said to be better suited for low-polarity compounds than DESI.

Since the idea behind ambient MS is to achieve high-throughput analysis, the sample preparation is usually kept to a minimum, and chromatographic separation is avoided. Under these conditions compounds originating from the matrix can increase the background signals (chemical noise) and make spectral interpretation difficult. Complex samples typically contain multiple compounds with only one or a few target analytes, and their response signals can be masked by signals from untargeted compounds. To alleviate spectral complexity without sacrificing the speed and simplicity of analysis, time-nested gas-phase separations based on ion mobility (IM) have been combined with ambient MS methods.[10,19–26] IM depends on the mass, charge, shape and size of the ions. In conventional ion mobility spectrometry (IMS), gas-phase ions are separated under the influence of a constant electric field, whereas in travelling wave ion mobility spectrometry (TWIMS) pulsed potential waves are passed through a drift chamber, where the separation of the ions takes place. When mobility-based separation techniques are combined with MS, the result is a powerful hyphenation resulting in higher peak capacity than can be achieved by stand-alone MS or IMS.[27–29]

Several ambient MS techniques have been coupled with IM separation techniques. DESI was first coupled with ion mobility mass spectrometry (IM-MS) for the analysis of proteins.[10] In another study, the charge-state distribution of tryptic peptides generated by DESI was determined via travelling wave ion mobility-mass spectrometry (TWIM-MS), with IM separation increasing the selectivity towards singly charged peptide ions, and simplifying the spectra.[21] DESI has also been combined with TWIM-MS for the rapid analysis of ingredients from pharmaceutical formulations.[19,20] In this case, the IM separation was observed to improve the spectral quality and the selectivity of the method for the compounds of interest. DESI and neutral desorption/extractive electrospray ionization (EESI) were used with TWIM-MS to study the active ingredients in pharmaceuticals, and to determine the collision cross-sections of polyethylene glycol ions.[22] DESI with TWIM-MS has also been used to develop a rapid ambient MS method for the analysis of chemical warfare agents.[23] More recently, DART has been coupled with a conventional stand-alone IMS, and its capability to analyze toxic chemicals was demonstrated.[25] Laser ablation/desorption electrospray ionization (LADESI) has also been combined with a stand-alone IMS instrument for the analysis of pharmaceutical tablets, providing fingerprints that distinguished counterfeit products from genuine ones.[26] To the best of our knowledge, DART has never been coupled with TWIM-MS, or DAPPI with any type of IMS.

The objective of this study was to couple DAPPI and DART with TWIM-MS to improve the spectrum interpretability and to increase the signal-to-noise ratio (S/N), while retaining the speed provided by ambient

Rapid Communications in Mass Spectrometry

MS. In addition, the sensitivities of DART and DAPPI for a variety of standards, and compounds from food and pharmaceutical products, are compared.

EXPERIMENTAL

Cholecalciferol (≥98%), benzo[a]pyrene (≥95%), bisphenol A (≥99%), ranitidine hydrochloride (≥99%), cortisol (≥98%) and toluene (HPLC grade, ≥99.9%) were purchased from Sigma-Aldrich (St. Louis, MO, USA). DL-α-tocopherol (≥99%) was from Merck (Darmstadt, Germany). Methanol (HPLC grade, 99.8+ %) and (≥99.9%) were purchased from Alfa Aesar (Ward Hill, MA, USA) and Sigma-Aldrich, respectively. Chloroform (HPLC grade, ≥99.8%) was purchased from EMD (Gibbstown, NJ, USA). Stock solutions of the studied compounds (5–30 mM) were prepared in methanol (bisphenol A, ranitidine, cortisol, α-tocopherol, cholecalciferol) or toluene (benzo[a]pyrene). The working solutions (1, 10 and 100 μM) were prepared in methanol or chloroform/methanol (1:1, v/v). Almonds and multivitamin tablets (One A Day, Bayer HealthCare LLC, Morristown, NJ, USA) were purchased from a local supermarket. Samples of genuine and fake levonorgestrel tablets (0.75 mg and 1.5 mg) were kindly provided by Paul N. Newton (Centre for Tropical Medicine, Churchill Hospital, University of Oxford, UK) and Dr. David Jenkins (FHI 360, USA), respectively. The content of the samples was previously verified at the Georgia Institute of Technology using multiple analytical platforms including DART and ESI-MS/MS with and without liquid chromatography (LC) separation and 2D DOSY ^{1}H NMR spectroscopy.[30] Dried blood spots, spiked with chloroquine, on Whatman filter paper were kindly provided by Dr. Michael D. Green (Center for Disease Control and Prevention (CDC), Atlanta, GA, USA). Chloroquine diphosphate salt (powder, purity ≥98%) used as standard was purchased from Sigma-Aldrich. The structures of the studied standards and compounds identified from the dried blood spots and pharmaceuticals are presented in Supplementary Fig. S1 (Supporting Information).

The experiments were carried out on a Synapt G2 HDMS (Waters Corp., Manchester, UK) in both MS and TWIM-MS modes. The operational parameters were optimized with benzo[a]pyrene and α-tocopherol using direct infusion μAPPI.[31] The Z-Spray ion source and the desolvation temperatures were set to 120 and 300 °C, respectively. The sampling and extraction cone voltages were 40 and 4.0 V, respectively. The TWIMS wave velocity was 583 m/s and wave height 35 V, unless otherwise mentioned. The data were acquired in positive ion mode. The MS data acquisition range was *m/z* 50–1000. The data was collected and processed with MassLynx version 4.1 and DriftScope version 2.1 (Waters Corp., Milford, MA, USA).

In DAPPI, a microchip heated nebulizer was used to deliver vaporized dopant and nebulizer gas towards the sampling surface. The DAPPI setup[14,15] and the manufacturing of the microchip and the chip holder[32] have been described in detail previously. The spray impact angle was approximately 45°. The microchip was heated using a programmable DC power supply (G W Instec, PSM-3004) operated at 4.4 W. The distance of the microchip nozzle from the sample spot, and the distance of the sample spot from the ceramic capillary inlet, were 4–5 and 3 mm, respectively. The PKR 100 VUV lamp (Heraeus Noblelight, Cambridge, UK), with 10.0 and 10.6 eV photon energy, was placed directly above the microchip nozzle, the sample spot and the inlet. The dopant was toluene at a flow rate of 10 μL/min. The nebulizer gas (nitrogen) flow rate was 180 mL/min. For the analysis of standard solutions, 1 μL samples were applied on a Teflon substrate (VINK Finland, Kerava, Finland) and left to dry. Four to eight spots per sample were analyzed in each experiment. Solid samples were held in front of the DAPPI solvent plume with tweezers.

A DART SVP ion source (IonSense, Inc., Saugus, MA, USA) was used for all DART experiments. The helium flow rate was 2.5 L/min and the discharge gas temperature was 250 °C in all experiments. The optimized distance between the ceramic DART exit nozzle (i.d. 4 mm) and the MS inlet was approximately 1 cm. The DART source was controlled via the DART SVP IonSense program. In DART experiments, 1 μL of a liquid sample was deposited on the tip of a melting point glass capillary and left to dry. The capillary tips were placed in front of the DART outlet nozzle to a distance of approximately 2 mm. Three to eight repeat injections were carried out for each sample. Solid pharmaceutical samples were held in front of the DART plasma plume with tweezers.

The Z-Spray ion source of the Synapt G2 HDMS instrument was fitted with a VAPUR gas-ion separator tube (GIST) interface (IonSense, Inc.), which enabled the use of both DAPPI and DART ion sources. In the interface, ions that are produced in the ionization region under atmospheric pressure conditions are suctioned through a ceramic capillary (i.d. 4 mm) into an enclosure that seals the modified Z-Spray source cone inlet. The neutrals are removed prior to entering the mass spectrometer by a model 2C diaphragm pump (Vacuubrand, Wertheim, Germany) attached to a gas outlet in the modified Z-Spray source cone inlet, the pumping rate of which was optimized for maximum ion detection.

RESULTS AND DISCUSSION

Comparison of DAPPI-MS and DART-MS

For comparison between DAPPI and DART, five selected standards: bisphenol A (BPA), benzo[a]pyrene (B[a]P), ranitidine, cortisol and α-tocopherol, were analyzed at concentrations of 1, 10 and 100 μM. All five standards were detected with both methods, but showed different fragment ions (Fig. 1) and displayed different sensitivities (Table 1). Table 1 summarizes the detected base peaks and the estimated limits of detection (LODs, the concentration where S/N = 3) achieved with each method. The LODs were extrapolated from the lowest experimentally detected concentration for the base peak of each compound.

Figures 1(a) and 1(b) show the mass spectra of BPA recorded using DAPPI and DART, respectively. Note, that a 100-times higher concentration was used to acquire the DART spectrum. With both ionization methods the base peak was observed at *m/z* 213, identified as the $[M–CH_3^{\bullet}]^+$ ion of BPA. With DAPPI, the $M^{+\bullet}$ at *m/z* 228 was also observed. The ion at *m/z* 213 was detected with high intensity with another MS instrument equipped with DAPPI as well (results not shown). The peak at *m/z* 229 can be either $[M+H]^+$ or possibly

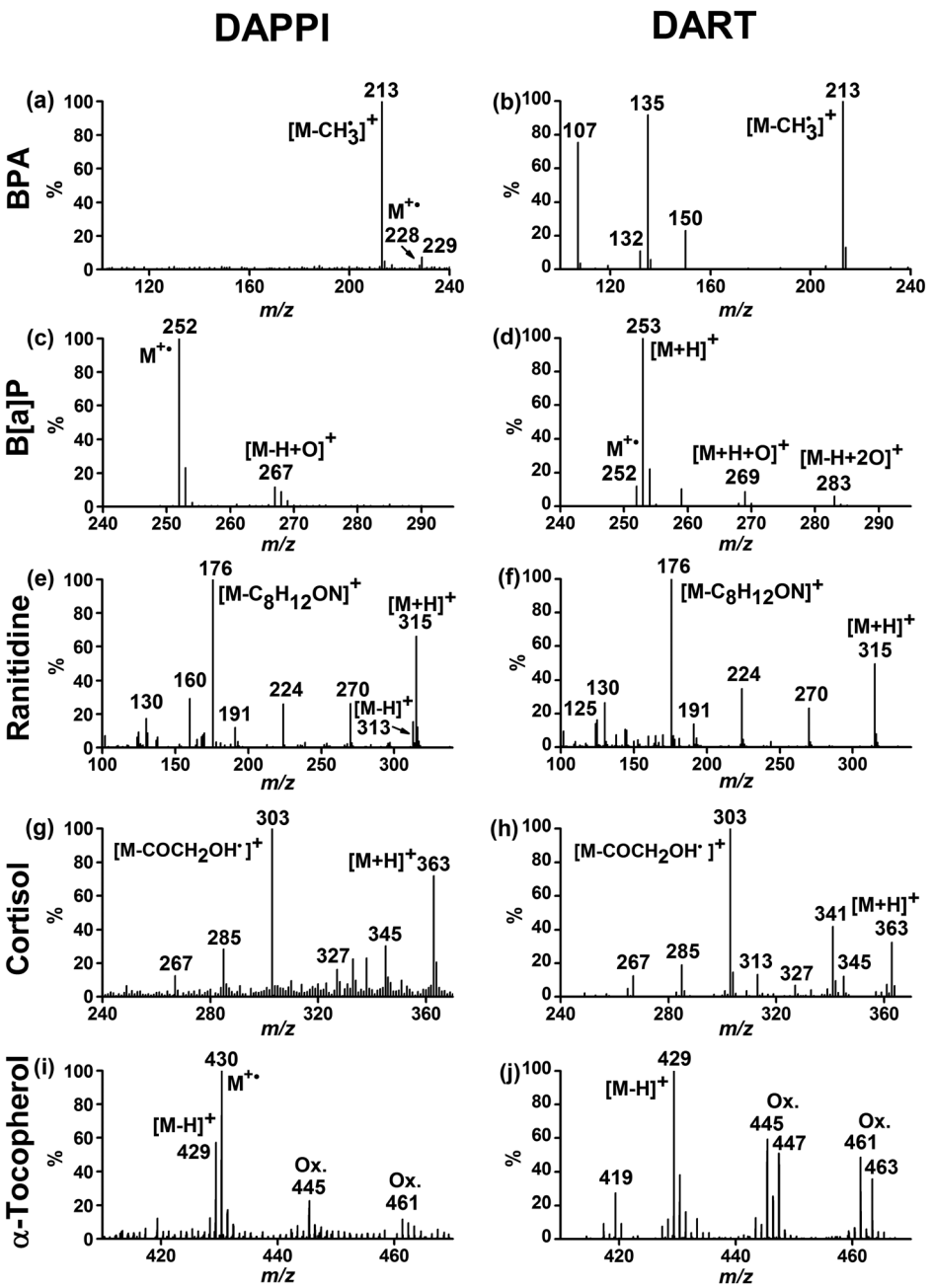

Figure 1. DAPPI and DART mass spectra of selected standards: (a) DAPPI of 1 μM BPA, (b) DART of 100 μM BPA, (c) DAPPI of 1 μM B[a]P, (d) DART of 10 μM B[a]P, (e) DAPPI of 10 μM ranitidine, (f) DART of 100 μM of ranitidine, (g) DAPPI of 1 μM cortisol, (h) DART of 10 μM cortisol, (i) DAPPI of 1 μM α-tocopherol, (j) DART of 10 μM α-tocopherol. Ox. in (i, j) corresponds to oxidation products. All the spectra have been background-subtracted.

an oxidation product, $[M–CH_3+O]^+$. These ions were not detected by DART for any of the tested concentrations, but instead fragments at *m/z* 107 and 135 were observed. A significant difference was observed in the sensitivity for BPA between DAPPI and DART with the extrapolated LODs reaching 90 fmol and 8.2 pmol, respectively. In the DART mass spectra, background ions were observed at *m/z* 55, 83, 101, 111, 129, 147, 259, 371 and 372, suspected to originate from the laboratory environment or the glass capillary used for sample introduction (not observed in the spectra in Fig. 1 due to background subtraction). With DAPPI, such ions were not observed. The reason for the higher background in DART may be the higher energy of He metastables compared to photons, which therefore can ionize a greater amount of background compounds.

B[a]P produced an abundant peak at 1 μM concentration with both ionization methods. In DAPPI, it was mainly ionized through charge exchange and detected as the $M^{+\bullet}$ ion at *m/z* 252, similarly to previous findings,[18] and as a possible oxidation product at *m/z* 267 ($[M–H+O]^+$) (Fig. 1(c)).

Rapid Communications in Mass Spectrometry

Table 1. Ions observed in DAPPI and DART, estimated LODs, and RSDs % (n = 3)

Compound	Base peak (*m/z*)	Estimated LOD (fmol)	RSD (%)
DAPPI			
Bisphenol A	$[M–CH_3^{\bullet}]^+$ (213)	90	8
Benzo[a]pyrene	$M^{+\bullet}$ (252)	30	9
Ranitidine	$[M–C_8H_{12}ON]^+$ (176)	290	33
Cortisol	$[M–COCH_2OH^{\bullet}]^+$ (303)	150	14
α-Tocopherol	$M^{+\bullet}$ (430)	190	28
DART			
Bisphenol A	$[M-CH_3^{\bullet}]^+$ (213)	8200	26
Benzo[a]pyrene	$[M+H]^+$ (253)	330	11
Ranitidine	$[M–C_8H_{12}ON]^+$ (176)	2500	11
Cortisol	$[M–COCH_2OH^{\bullet}]^+$ (303)	920	37
α-Tocopherol	$[M–H]^+$ (429)	3200	19

With DART, the main peak of B[a]P was the $[M+H]^+$ ion (Fig. 1(d)) at *m/z* 253; in addition, oxidation product ions of type $[M+H+O]^+$ and $[M–H+2O]^+$ at *m/z* 269 and 283, respectively, were also observed. Also, the $M^{+\bullet}$ ion of B[a]P, possibly generated through Penning ionization by the He metastables, was observed in the DART mass spectrum with an intensity approximately 15% of that of the $[M+H]^+$ ion. Rummel *et al.* have reported that PAH compounds can be ionized by DART as both $M^{+\bullet}$ and $[M+H]^+$ ions, depending on the distance between the sample and the DART source exit, with positions closer to the DART exit resulting in a higher proportion of $M^{+\bullet}$ ions.[33] In the present study the extrapolated LODs for B[a]P were 30 and 330 fmol for DAPPI and DART, respectively.

For ranitidine, an ion at *m/z* 176 was observed as the main peak with both DAPPI and DART (Figs. 1(e) and 1(f)), tentatively identified as a fragment of type $[M–C_8H_{12}ON]^+$. Also, an abundant $[M+H]^+$ ion at *m/z* 315 was detected with both techniques, as well as fragment ions at *m/z* 130, 191, 224 and 270. Fragment ions at *m/z* 138 and 160, and a hydride abstraction product $[M–H]^+$ at *m/z* 313, were detected with DAPPI, but not with DART. Ranitidine contains several nitrogen atoms, which increase its PA and enable efficient ionization through proton transfer. With DART, ranitidine has been previously detected from urine as the $[M+H]^+$ ion, but the concentration was not reported.[3] Weston *et al.* analyzed ranitidine from Zantac 75 tablets with DESI coupled with IM-MS and reported a LOD of 630 pmol.[19] Here, the extrapolated LODs for ranitidine were 290 fmol and 2.5 pmol with DAPPI and DART, respectively (Table 1), meaning that approximately 2200 and 250 times higher sensitivity was reached in our study.

For cortisol, the main peak with both DAPPI and DART was observed at *m/z* 303, suggested to originate from cleavage of $-COCH_2OH^{\bullet}$ from $M^{+\bullet}$ (Figs. 1(g) and 1(h)).[34] This finding was supported by later DAPPI-MS studies, where the ion at *m/z* 303 was detected with high intensity, although the $M^{+\bullet}$ of cortisol was not observed; and MS/MS studies from the cortisol $[M+H]^+$, which showed no trace of *m/z* 303 (results not shown). In the present study, the $[M+H]^+$ ion at *m/z* 363 was detected with both techniques. Dehydration products from the $[M+H]^+$ and the $[M–COCH_2OH^{\bullet}]^+$ ions were observed at *m/z* 327 ($[M+H–H_2O]^+$) and 345 ($[M+H–2H_2O]^+$), and at *m/z* 285 ($[M–COCH_2OH^{\bullet}–H_2O]^+$) and 267 ($[M–COCH_2OH^{\bullet}–2H_2O]^+$), respectively. For cortisol, the detected ions and their relative intensities were almost identical in DAPPI and DART, the main difference was in the observed sensitivity: for 10 μM sample concentration, the S/N was four times higher with DAPPI than with DART. The estimated LODs with DAPPI and DART were 150 and 920 fmol, respectively (Table 1, corresponding to 150 and 920 nM concentration, respectively, for a 1 μL sample). A 5.5 nM LOD for cortisol has been reported in a previous DART-MS study, where the sampling was done by dipping the sample probe into a sample solution (this is likely to result in a larger overall sample volume than used in this study).[35] Jorabchi *et al.* have reported the analysis of cortisol using DART and photoionization, in a setup somewhat similar to DAPPI.[36] They analyzed 6 ng of sample, corresponding to 17 pmol of cortisol, but the LOD was not reported.

α-Tocopherol was detected with DAPPI from a 1 μM sample solution as an abundant $M^{+\bullet}$ ion at *m/z* 430 and as the $[M–H]^+$ ion at *m/z* 429 (Fig. 1(i)). Oxidation products at *m/z* 445 ($[M–H+O]^+$) and 461 ($[M–H+2O]^+$) were also observed. With DART, the main peak of α-tocopherol at 10 μM concentration was the $[M–H]^+$ ion (Fig. 1(j)); in addition, oxidation products at *m/z* 445, 447, 461, and 463 were observed. The estimated LODs for α-tocopherol with DAPPI and DART were 190 fmol and 3.2 pmol, respectively (Table 1). In an earlier study, α-tocopherol was detected as the $M^{+\bullet}$ ion with DAPPI from a 10 μM sample, but the LOD was not reported.[11] In the same study, much lower ionization efficiency for α-tocopherol was achieved with DESI, because of the non-polar nature of the compound. Analysis of α-tocopherol with DART has not been reported in the literature, to the best of our knowledge.

Surface analysis using DAPPI-TWIM-MS and DART-TWIM-MS

Analysis of a chloroquine-spiked blood sample

Chloroquine is an antimalarial drug, which has previously been analyzed with DESI-MS directly from tablets.[37] Here, the feasibilities of DAPPI and DART for the rapid and direct analysis of chloroquine from dried blood spots on filter paper (10 μL of human blood with 3 μM chloroquine) were investigated.

Chloroquine was detected by both DAPPI-MS and DART-MS as the $[M+H]^+$ ion at *m/z* 320 (Figs. 2(a) and 2(b)). DAPPI showed eight times higher ionization efficiency and 14 times higher S/N when compared with DART. In addition to the $[M+H]^+$ion, a typical fragment of chloroquine $[M–C_4H_{11}N]^+$ at *m/z* 247 was observed in the DAPPI spectrum. In both DAPPI and DART spectra, ions at *m/z* 385, 367, 401 and 417 were also observed, thought to be $[M–H]^+$,[11,12] $[M–H–H_2O]^+$, $[M–H+O]^+$ and $[M–H+2O]^+$, respectively, of blood cholesterol.

In order to clean up the DART mass spectrum from interfering agents and to improve the detection of chloroquine, DART analysis with TWIM separation was investigated. Figures 2(c) and 2(d) show the total IM spectrum of all the ions produced from the blood sample by DART, and the combined mass spectrum from the total IM data, respectively. The chloroquine ion at *m/z* 320 is not clearly observed in the combined mass spectrum in Fig. 2(d). Figure 2(e), however, presents the single IM spectrum of the ion at *m/z* 320 with a drift time at 3.9 ms. The mass spectrum extracted from the single chloroquine IM spectrum is shown in Fig. 2(f), with a significantly higher relative abundance for the $[M+H]^+$ ion.

DAPPI- and DART-TWIM-MS surface analysis of almond

The coupling of TWIM separation to DAPPI-MS and DART-MS was also demonstrated by the analysis of α-tocopherol directly from almond surface. Figures 3(a) and 3(b) show

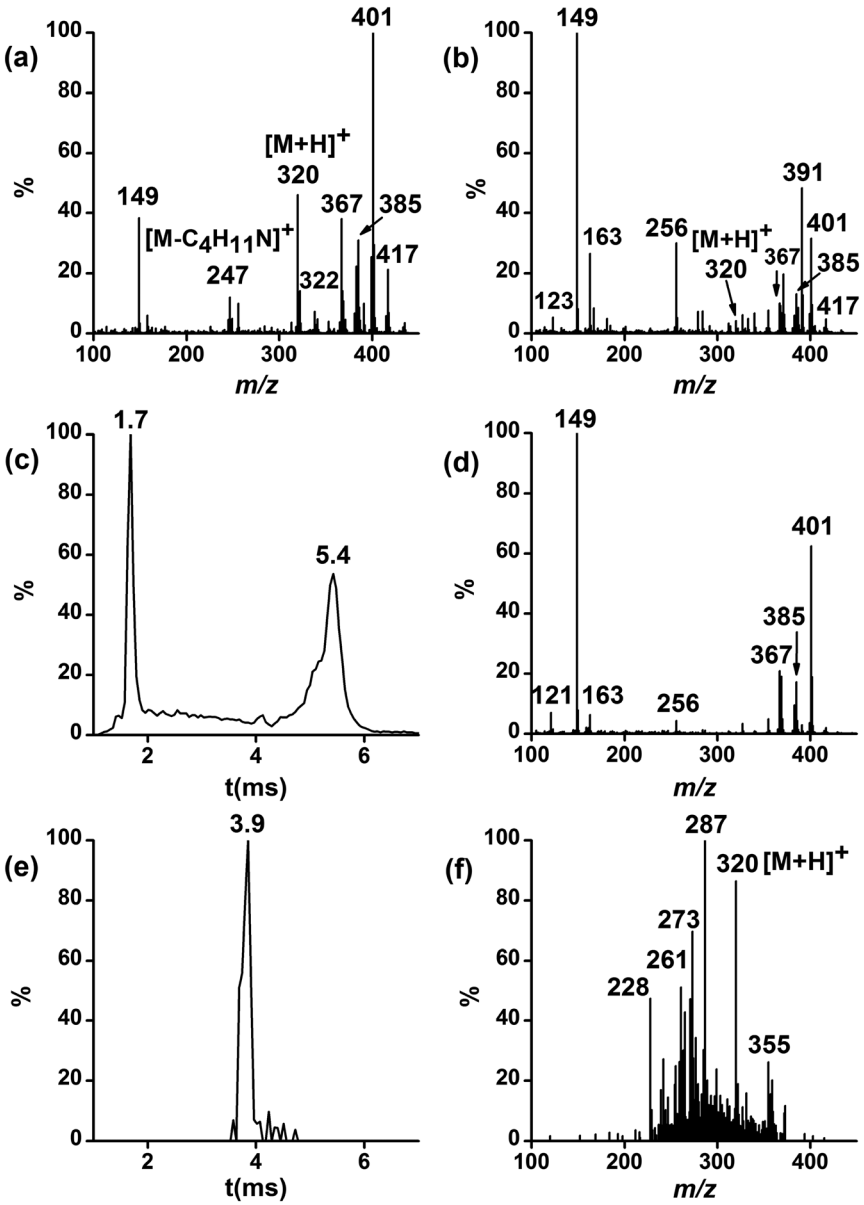

Figure 2. (a) DAPPI-MS, (b) DART-MS and (c–f) DART-TWIM-MS analysis of a dried blood spot spiked with chloroquine (detected as the $[M+H]^+$ ion at *m/z* 320). (c) DART-TWIM-MS total IM spectrum of the dried blood spot, (d) combined mass spectrum from the total IM data in (c), (e) single IM spectrum of $[M+H]^+$ ion of chloroquine at *m/z* 320, (f) combined mass spectrum from the IM data in (e). The ion at *m/z* 149 is background.

Rapid Communications in Mass Spectrometry

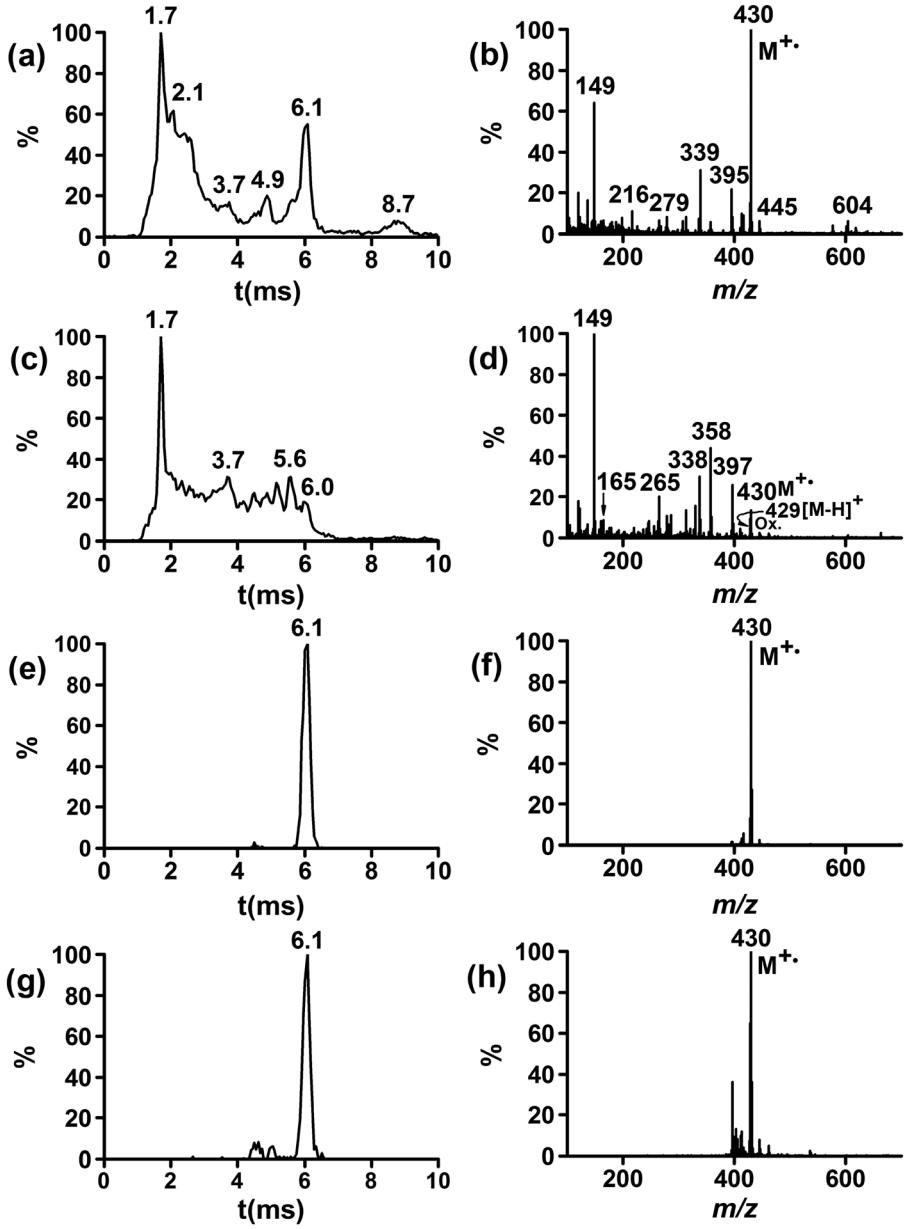

Figure 3. DAPPI- and DART-TWIM-MS of almond surface: (a) DAPPI-TWIM-MS total IM spectrum, (b) combined mass spectrum from the total IM data in (a), (c) DART-TWIM-MS total IM spectrum, (d) combined mass spectrum from the total IM data in (c) (Ox. corresponds to oxidation products at *m/z* 445, 447 and 462), (e) single DAPPI-IM spectrum of $M^{+\bullet}$ ion of α-tocopherol at *m/z* 430, (f) combined mass spectrum from the IM data in (e), (g) single DART-IM spectrum of the $M^{+\bullet}$ ion of α-tocopherol at *m/z* 430, (h) combined mass spectrum from the IM data in (g).

the total IM spectrum, and the combined mass spectrum from the total IM data of all the ions produced, respectively, from almond surface by positive ion DAPPI. Figures 3(c) and 3(d) show the corresponding DART data. With both methods, the $M^{+\bullet}$ ion of α-tocopherol at *m/z* 430 was detected. In addition, an oxidation product $[M–H+O]^+$ at *m/z* 445 was observed with DAPPI. With DART, the $[M–H]^+$ at *m/z* 429, a fragment at *m/z* 165, and oxidation products at *m/z* 445 ($[M–H+O]^+$), 447 ($[M+H+O]^+$) and 462 ($[M+2O]^+$) were also detected. Identification of α-tocopherol was verified by comparison with standards. Figures 3(e) and 3(f) show the single IM spectrum of the $M^{+\bullet}$ ion of α-tocopherol obtained with DAPPI, and the combined mass spectrum of the single IM data, respectively. Corresponding data for DART are presented in Figs. 3(g) and 3(h). With both DAPPI and DART, the single IM spectra showed the same drift time of 6.1 ms for the $M^{+\bullet}$ ion of α-tocopherol. As can be observed from the mobility-separated mass spectra in Figs. 3(f) and 3(h), the IM separation prior to MS analysis greatly reduced the chemical noise in the acquired mass spectrum. Especially for DART, which gave lower signal intensity for α-tocopherol than DAPPI, the mobility-filtered spectral data provided approximately 27 times higher S/N for the $M^{+\bullet}$ ion of α-tocopherol than obtained from MS data alone.

DAPPI-TWIM-MS of vitamin products and pharmaceuticals

Since as shown above DAPPI proved to be more sensitive than DART for the selected compounds, it was chosen for further studies, where the suitability of the TWIMS in the analysis of authentic samples with ambient MS was investigated.

DAPPI-TWIM-MS screening of a multivitamin tablet

DAPPI-TWIM-MS was used to analyze the ingredients in a multivitamin product containing several vitamins, minerals, and excipients (Supplementary Table S1, Supporting Information). Seven out of thirteen vitamins reported by the product manufacturer were detected. Figures 4(a) and 4(b) show the total IM spectrum and the combined mass spectrum

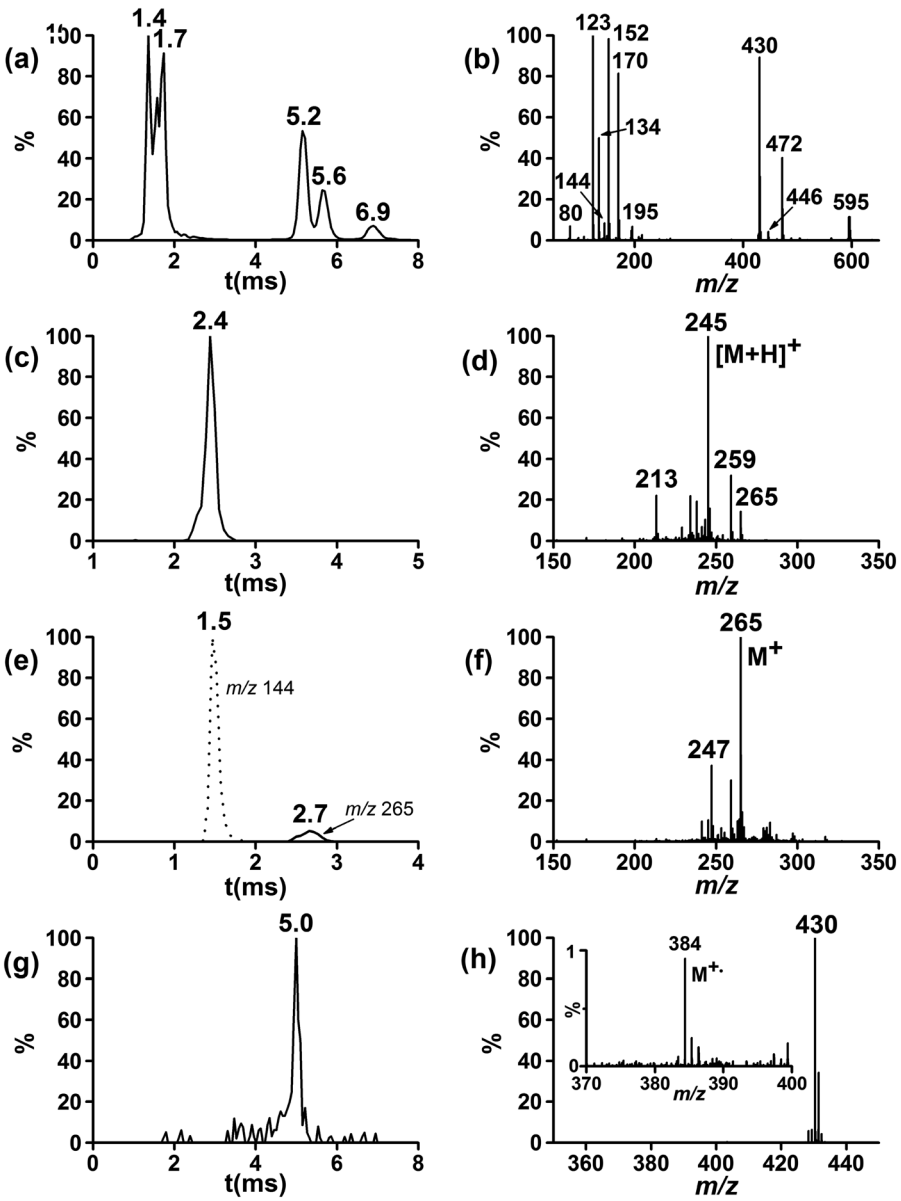

Figure 4. DAPPI-TWIM-MS analysis of the scratched surface of a multivitamin tablet: (a) total IM spectrum, (b) combined mass spectrum from the total IM data, where the ion at *m/z* 123 is $[M+H]^+$ of nicotinamide, 170 is $[M+H]^+$ of pyridoxine, 195 is $[M+H]^+$ of caffeine, 430 is $M^{+\bullet}$ of α-tocopherol and 472 is $[M+H]^+$ of α-tocopheryl acetate, (c) single IM spectrum for biotin $[M+H]^+$ at *m/z* 245, (d) combined mass spectrum from the IM data in (c), (e) single IM spectrum for the thiamine M^+ ion at *m/z* 265 (and for thiamine fragment ion at *m/z* 144 with dashed line), (f) combined mass spectrum from the IM data in (e), (g) single IM spectrum for the cholecalciferol $M^{+\bullet}$ at *m/z* 384, (h) combined mass spectrum from IM data in (g) (insert shows enlargement of the spectrum from mass range *m/z* 370–400). The TWIMS wave velocity was 530 m/s and wave height 35 V.

Rapid Communications in Mass Spectrometry

from the total IM data, respectively. The main peaks observed in the multivitamin tablet were due to nicotinamide (amide of niacin, vitamin B_3, $[M+H]^+$ at *m/z* 123), pyridoxine (vitamin B_6, $[M+H]^+$, and dehydration products $[M+H-H_2O]^+$ and $[M+H-2H_2O]^+$ at *m/z* 170, 152 and 134, respectively) and α-tocopherol ($M^{+\bullet}$, oxidation product $[M+O]^+$ and α-tocopheryl acetate at *m/z* 430, 446 and 472, respectively), as shown in Fig. 4(b). The $[M+H]^+$ ion of caffeine was observed at *m/z* 195. Supplementary Fig. S2 (Supporting Information) presents the single IM spectra of protonated pyridoxine and its dehydration products, where the mild tailing observed for the peaks is possibly due to dissociation in the drift region.

In addition, less intense peaks that were due to biotin (vitamin B_7), thiamine (vitamin B_1) and cholecalciferol (vitamin D_3) were observed. The single IM spectra and the corresponding combined mass spectra for these three vitamins are presented in Figs. 4(c)–4(h). Biotin (Figs. 4(c) and 4(d)) was detected as the $[M+H]^+$ at *m/z* 245, for which the single IM spectrum showed a narrow peak at a drift time of 2.4 ms. Thiamine was detected as the $M^{+\bullet}$ ion at *m/z* 265 with a drift time of 2.7 ms (Figs. 4(e) and 4(f)). The ion at *m/z* 144 (Fig. 4(b)) was identified as the thiamine fragment ion $[M-C_6H_7N_3]^+$, for which the mobility spectrum is also presented in Fig. 4(e). Cholecalciferol was detected as the $M^{+\bullet}$ ion at *m/z* 384 with a drift time of 5.0 ms (Figs. 4(g) and 4(h); assignment verified by analyzing standards). The single IM spectrum of the cholecalciferol $M^{+\bullet}$ ion partly overlapped the highly abundant signal of α-tocopherol at *m/z* 430, due to the high concentration of α-tocopherol in the sample (25 mg, see Supplementary Table S1, Supporting Information), and a resulting wide signal in the TWIMS spectrum. Figure 4(h) shows the combined mass spectrum from the single IM data of the cholecalciferol $M^{+\bullet}$ ion, with an insert showing enlargement of the *m/z* 370–400 range. The concentration of α-tocopherol in the vitamin product was 1500 times higher than the concentration of cholecalciferol (0.01 mg), which explains why the intensity of the cholecalciferol ion peak is low compared to α-tocopherol. The S/N was seven times higher when the mobility separation was utilized compared to the case when it was not, which demonstrates how the

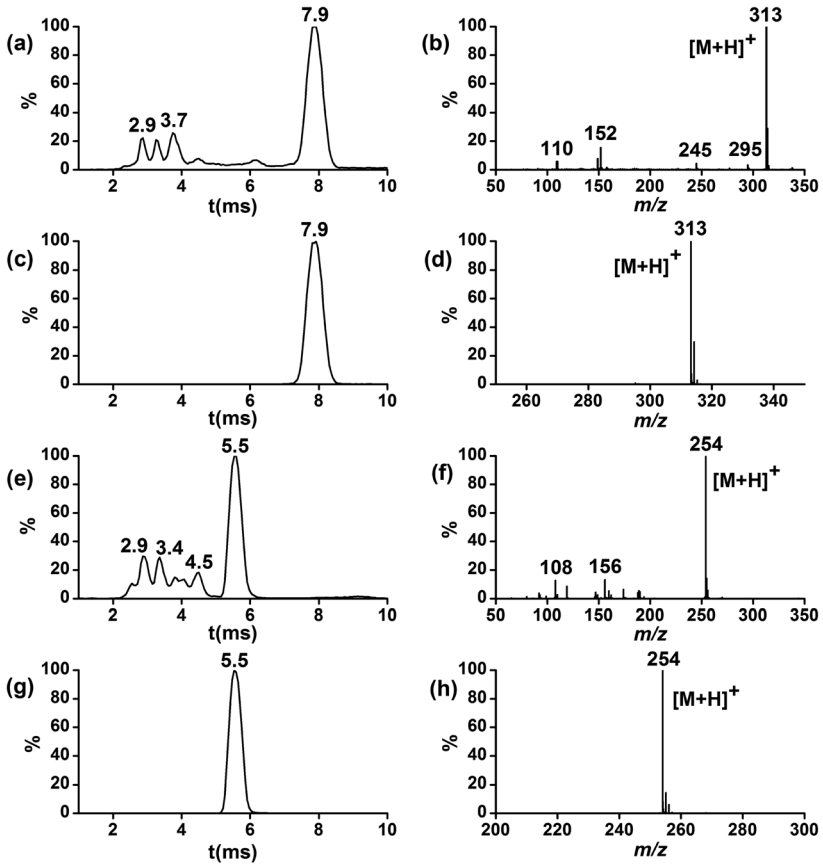

Figure 5. DAPPI-TWIM-MS analysis from the surface of authentic and potentially falsified levonorgestrel tablets: (a) total IM spectrum from the authentic tablet, (b) combined mass spectrum from the total IM data in (a), (c) single IM spectrum of the $[M+H]^+$ of levonorgestrel at *m/z* 313 detected from the authentic tablet, (d) combined mass spectrum from the IM data in (c), (e) total IM spectrum from a potentially falsified tablet, (f) combined mass spectrum from the total IM data in (e), (g) single IM spectrum of the $[M+H]^+$ ion of sulfamethoxazole at *m/z* 254 detected from the falsified tablet, (h) combined mass spectrum from the IM data in (g). The TWIMS wave velocity was 600 m/s and wave height 24 V.

mobility separation significantly increased S/N and helped to distinguish low-intensity cholecalciferol $M^{+\bullet}$ from other compounds.

Detection of both water- and fat-soluble vitamins, with high intensities, demonstrates the potential of DAPPI-MS for the analysis of both polar as well as non-polar compounds. Some vitamins reported in the vitamin product were not detected under the experimental conditions of the current study. Negative mode MS and/or solvent modification could probably facilitate the detection of acidic compounds (ascorbic acid and folic acid), photodegradable compounds (retinol and β-carotene), high molecular weight compounds (cyanocobalamin), and certain water-soluble nitrogen-containing compounds (riboflavin).

DAPPI-TWIM-MS for screening pharmaceutical tablets

Ambient MS analysis is an effective tool for the rapid screening of active ingredients in pharmaceutical formulations.[1,3,19,24,38] However, sample matrices can be complex and usually contain excipient compounds, which can interfere with ionization or identification of chemicals of interest. Here, TWIMS was used as a fast gas-phase separation technique before MS to reduce chemical noise in the mass spectra, when genuine emergency contraceptive tablets containing levonorgestrel, and falsified tablets, sold as genuine, were analyzed by DAPPI-TWIM-MS. Figures 5(a) and 5(b) show the total IM spectrum of all ions produced from a genuine pharmaceutical tablet containing levonorgestrel, and the combined mass spectrum from the total IM data, respectively. Levonorgestrel can be observed with high abundance as the $[M+H]^+$ ion at *m/z* 313. Figure 5(c) presents the single IM spectrum of the levonorgestrel $[M+H]^+$ ion, showing that the levonorgestrel drift time, 7.9 ms, corresponds to the high intensity peak in the total IM spectrum. Figure 5(d) presents the combined mass spectrum from the $[M+H]^+$ levonorgestrel single IM spectrum. The mobility separation was observed to remove the background from the mass spectrum, allowing the detection of the target compound with increased selectivity. The total IM spectrum and the corresponding combined mass spectrum of the potentially falsified tablet are illustrated in Figs. 5(e) and 5(f), respectively. The DAPPI-TWIM-MS analysis showed no evidence of levonorgestrel in the tablet, but, instead, the main ingredient was detected at a drift time of 5.5 ms and at *m/z* 254, as shown in the single IM spectrum of the ion at *m/z* 254 and the corresponding combined mass spectrum in Figs. 5(g) and 5(h), respectively. This species was identified as the $[M+H]^+$ ion of the antibiotic sulfamethoxazole with typical fragments at *m/z* 156 and 108 (Fig. 5(f) and Supplementary Fig. S3, Supporting Information). Identification of the wrong active ingredient present in the suspect formulation was previously achieved using a tiered analytical platform.[30] DAPPI-TWIM-MS results agreed well with previous results. Supplementary Figs. S3(a)–S3(d) (Supporting Information) show the single IM spectra and the corresponding combined mass spectra of the sulfamethoxazole $[M+H]^+$ fragment ions at *m/z* 156 and 108. The insert in Supplementary Fig. S3(a) shows an enlargement from the relative abundance range of 0–1% of Supplementary Fig. S3(a). It shows how the ion at *m/z* 156 has partly formed most likely from the sulfamethoxazole $[M+H]^+$ ion during and after the mobility separation before the MS analysis. Also the tailing of the ion at *m/z* 108 (Supplementary Fig. S3(c)) indicates that some of the ions underwent dissociation in the drift tube.

CONCLUSIONS

In this work we reported the successful coupling of both DAPPI and DART with TWIM-MS, and showed how ions could be totally or partly separated from the background noise by their different mobilities in the drift region, and how this separation enhanced spectral quality and S/N. The ambient MS techniques DAPPI and DART were compared, and DAPPI was shown to be more sensitive than DART for a small group of standard compounds, and the pharmaceutical chloroquine, which was analyzed directly from a dried blood spot. The background observed in DART was higher in all examples, which partly explains the lower S/N. A more comprehensive study on the different features of DAPPI and DART is necessary before making final conclusions, but since the analytes studied here contained both polar and nonpolar compounds, the results are likely to indicate a general trend.

A challenge in the field of ambient MS is interference by background substances during direct ionization, which in the case of complex samples may hide the signals of the analytes of interest. Therefore, there is need for fast separation methods that do not increase the analysis time and thus remove the advantage of speed of ambient MS. For DAPPI, this was the first time that IM separation was used as a separation technique prior to MS analysis. This combination of analytical devices can have important applications in e.g. screening analysis of pharmaceuticals, illicit drugs, toxic chemicals or explosives from tablets, biological matrices, environmental samples and food products. Especially in cases where the analyte concentration is close to the detection limit and the number of matrix components is high, the IM separation can be expected to improve the information content that can be achieved from a particular sample. More studies in the coupling of DAPPI with different types of IM separators are still needed to achieve a full picture of the capabilities of DAPPI-IM-MS.

Acknowledgements

The Academy of Finland (Projects 125758, 218150 and 255559) and CHEMSEM Graduate School are acknowledged for financial support. Markus Haapala is thanked for manufacturing the microchip heated nebulizers and Joel Keelor (JK) for assistance in the laboratory. Paul Newton and David Jenkins (University of Oxford, Oxford, UK and FHI 360 USA) are acknowledged for providing the genuine and fake levonorgestrel tablets. Michael D. Green (Center for Disease Control and Prevention (CDC), Atlanta, GA, USA) is acknowledged for providing the dried chloroquine spiked blood samples. FMF, JK and PD acknowledge support from the NSF and NASA Astrobiology Program under the NSF Center for Chemical Evolution (CHE-1004570). PD acknowledges partial financial support from a research contract with Photonis USA.

Rapid Communications in Mass Spectrometry

REFERENCES

[1] M.E. Monge, G.A. Harris, P. Dwivedi, F.M. Fernández. Mass spectrometry: recent advances in direct open air surface sampling/ionization. *Chem. Rev.* **2013**, *113*, 2269.

[2] Z. Takáts, J.M. Wiseman, B. Gologan, R.G. Cooks. Mass spectrometry sampling under ambient conditions with desorption electrospray ionization. *Science* **2004**, *306*, 471.

[3] R.B. Cody, J.A. Laramée, H.D. Durst. Versatile new ion source for the analysis of materials in open air under ambient conditions. *Anal. Chem.* **2005**, *77*, 2297.

[4] A. Venter, P.E. Sojka, R.G. Cooks. Droplet dynamics and ionization mechanisms in desorption electrospray ionization mass spectrometry. *Anal. Chem.* **2006**, *78*, 8549.

[5] A.B. Costa, R.G. Cooks. Simulation of atmospheric transport and droplet-thin film collisions in desorption electrospray ionization. *Chem. Commun.* **2007**, 3915.

[6] J.V. Iribarne, B.A. Thomson. On the evaporation of small ions from charged droplets. *J. Chem. Phys.* **1976**, *64*, 2287.

[7] B.A. Thomson, J.V. Iribarne. Field-induced ion evaporation from liquid surfaces at atmospheric pressure. *J. Chem. Phys.* **1979**, *71*, 4451.

[8] M. Dole, L.L. Mack, R.L. Hines, R.C. Mobley, L.D. Ferguson, M.B. Alice. Molecular beams of macroions. *J. Chem. Phys.* **1968**, *49*, 2240.

[9] Z. Takáts, J.M. Wiseman, R.G. Cooks. Ambient mass spectrometry using desorption electrospray ionization (DESI): Instrumentation, mechanisms and applications in forensics, chemistry, and biology. *J. Mass Spectrom.* **2005**, *40*, 1261.

[10] S. Myung, J.M. Wiseman, S.J. Valentine, Z. Takáts, R.G. Cooks, D.E. Clemmer. Coupling desorption electrospray ionization with ion mobility/mass spectrometry for analysis of protein structure: evidence for desorption of folded and denatured states. *J. Phys. Chem. B.* **2006**, *110*, 5045.

[11] N.M. Suni, H. Aalto, T.J. Kauppila, T. Kotiaho, R. Kostiainen. Analysis of lipids with desorption atmospheric pressure photoionization-mass spectrometry (DAPPI-MS) and desorption electrospray ionization-mass spectrometry (DESI-MS). *J. Mass Spectrom.* **2012**, *47*, 611.

[12] R.B. Cody. Observation of molecular ions and analysis of nonpolar compounds with the direct analysis in real time ion source. *Anal. Chem.* **2009**, *81*, 1101.

[13] L. Song, S.C. Gibson, D. Bhandari, K.D. Cook, J.E. Bartmess. Ionization mechanism of positive-ion direct analysis in real time: a transient microenvironment concept. *Anal. Chem.* **2009**, *81*, 10080.

[14] M. Haapala, J. Pól, V. Saarela, V. Arvola, T. Kotiaho, R.A. Ketola, S. Franssila, T.J. Kauppila, R. Kostiainen. Desorption atmospheric pressure photoionization. *Anal. Chem.* **2007**, *79*, 7867.

[15] L. Luosujärvi, V. Arvola, M. Haapala, J. Pól, V. Saarela, S. Franssila, T. Kotiaho, R. Kostiainen, T.J. Kauppila. Desorption and ionization mechanisms in desorption atmospheric pressure photoionization. *Anal. Chem.* **2008**, *80*, 7460.

[16] A. Vaikkinen, M. Haapala, H. Kersten, T. Benter, R. Kostiainen, T.J. Kauppila. Comparison of direct and alternating current vacuum ultraviolet lamps in atmospheric pressure photoionization. *Anal. Chem.* **2012**, *84*, 1408.

[17] N.M. Suni, P. Lindfors, O. Laine, P. Östman, I. Ojanperä, T. Kotiaho, T.J. Kauppila, R. Kostiainen. Matrix effect in the analysis of drugs of abuse from urine with desorption atmospheric pressure photoionization-mass spectrometry (DAPPI-MS) and desorption electrospray ionization-mass spectrometry (DESI-MS). *Anal. Chim. Acta.* **2011**, *699*, 73.

[18] L. Luosujärvi, S. Kanerva, V. Saarela, S. Franssila, R. Kostiainen, T. Kotiaho, T.J. Kauppila. Environmental and food analysis by desorption atmospheric pressure photoionization-mass spectrometry *Rapid Commun Mass Spectrom.* **2010**, *24*, 1343.

[19] D.J. Weston, R. Bateman, I.D. Wilson, T.R. Wood, C.S. Creaser. Direct analysis of pharmaceutical drug formulations using ion mobility spectrometry/quadrupole-time-of-flight mass spectrometry combined with desorption electrospray ionization. *Anal. Chem.* **2005**, *77*, 7572.

[20] E.L. Harry, J.C. Reynolds, A.W.T. Bristow, I.D. Wilson, C.S. Creaser. Direct analysis of pharmaceutical formulations from non-bonded reversed-phase thin-layer chromatography plates by desorption electrospray ionisation ion mobility mass spectrometry. *Rapid Commun. Mass Spectrom.* **2009**, *23*, 2597.

[21] G. Kaur-Atwal, D.J. Weston, P.S. Green, S. Crosland, P.L.R. Bonner, C.S. Creaser. Analysis of tryptic peptides using desorption electrospray ionisation combined with ion mobility spectrometry/mass spectrometry. *Rapid Commun. Mass Spectrom.* **2007**, *21*, 1131.

[22] J.P. Williams, J.H. Scrivens. Coupling desorption electrospray ionization and neutral desorption/extractive electrospray ionization with a travelling-wave based ion mobility mass spectrometer for the analysis of drugs. *Rapid Commun. Mass Spectrom.* **2008**, *22*, 187.

[23] P.A. D'Agostino, C.L. Chenier. Desorption electrospray ionization mass spectrometric analysis of organophosphorus chemical warfare agents using ion mobility and tandem mass spectrometry. *Rapid Commun. Mass Spectrom.* **2010**, *24*, 1617.

[24] A.S. Galhena, G.A. Harris, M. Kwasnik, F.M. Fernández. Enhanced direct ambient analysis by differential mobility-filtered desorption electrospray ionization-mass spectrometry. *Anal. Chem.* **2010**, *82*, 9159.

[25] G.A. Harris, M. Kwasnik, F.M. Fernández. Direct analysis in real time coupled to multiplexed drift tube ion mobility spectrometry for detecting toxic chemicals. *Anal. Chem.* **2011**, *83*, 1908.

[26] G.A. Harris, S. Graf, R. Knochenmuss, F.M. Fernández. Coupling laser ablation/desorption electrospray ionization to atmospheric pressure drift tube ion mobility spectrometry for the screening of antimalarial drug quality. *Analyst* **2012**, *137*, 3039.

[27] A.B. Kanu, P. Dwivedi, M. Tam, L. Matz, H.H. Hill Jr. Ion mobility-mass spectrometry. *J. Mass Spectrom.* **2008**, *43*, 1.

[28] C. Lapthorn, F. Pullen, B.Z. Chowdhry. Ion mobility spectrometry-mass spectrometry (IMS-MS) of small molecules: Separating and assigning structures to ions. *Mass Spectrom. Rev.* **2013**, *32*, 43.

[29] P. Dwivedi, G. Puzon, M. Tam, D. Langlais, S. Jackson, K. Kaplan, W.F. Siems, A.J. Schultz, L. Xun, A. Woods, H.H. Hill Jr. Metabolic profiling of *Escherichia coli* by ion mobility-mass spectrometry with MALDI ion source. *J. Mass Spectrom.* **2010**, *45*, 1383.

[30] M.E. Monge, P. Dwivedi, M. Zhou, F.M. Fernández, M. Payne, C. Harris, B. House, Y. Juggins, P. Cizmarik, D. Jenkins, P.N. Newton. A tiered analytical approach for investigating poor quality emergency contraceptives *PLoS One* **2014**, *9*, e95353.

[31] T.J. Kauppila, P. Östman, S. Marttila, R.A. Ketola, T. Kotiaho, S. Franssila, R. Kostiainen. Atmospheric pressure photoionization-mass spectrometry with a microchip heated nebulizer. *Anal. Chem.* **2004**, *76*, 6797.

[32] V. Saarela, M. Haapala, R. Kostiainen, T. Kotiaho, S. Franssila. Glass microfabricated nebulizer chip for mass spectrometry. *Lab Chip.* **2007**, *7*, 644.
[33] J.L. Rummel, A.M. McKenna, A.G. Marshall, J.R. Eyler, D.H. Powell. The coupling of direct analysis in real time ionization to Fourier transform ion cyclotron resonance mass spectrometry for ultrahigh-resolution mass analysis. *Rapid Commun. Mass Spectrom.* **2010**, *24*, 784.
[34] J. Van der Greef, N.M.M. Nibbering. Detection of unimolecular gas phase decompositions of ions, generated upon field desorption, in the time range of 10^{-11}-10^{-9}. *Int. J. Mass Spectrom. Ion Phys.* **1977**, *25*, 357.
[35] Y. Zhao, M. Lam, D. Wu, R. Mak. Quantification of small molecules in plasma with direct analysis in real time tandem mass spectrometry, without sample preparation and liquid chromatographic separation. *Rapid Commun. Mass Spectrom.* **2008**, *22*, 3217.
[36] K. Jorabchi, K. Hanold, J. Syage. Ambient analysis by thermal desorption atmospheric pressure photoionization. *Anal. Bioanal. Chem.* **2013**, *405*, 7011.
[37] L. Nyadong, A.S. Galhena, F.M. Fernández. Desorption electrospray/metastable-induced ionization: a flexible multimode ambient ion generation technique. *Anal. Chem.* **2009**, *81*, 7788.
[38] M.J. Culzoni, P. Dwivedi, M.D. Green, P.N. Newton, F.M. Fernández. Ambient mass spectrometry technologies for the detection of falsified drugs. *MedChemComm.* **2014**, *5*, 9.

SUPPORTING INFORMATION

Additional supporting information may be found in the online version of this article at the publisher's website.

